FINAL REVISION OF THE STEADY STATE INTERACTION OF RISING MAGMA WITHIN DRIFTS: SUMMARY REPORT OF MAGMA FLOW DYNAMICS IN THE POTENTIAL YUCCA MOUNTAIN REPOSITORY FROM EXPERIMENTAL STUDIES PERFORMED AT THE UNIVERSITY OF BRISTOL, BRISTOL, UNITED KINGDOM

Prepared for

U.S. Nuclear Regulatory Commission
Contract NRC–02–07–006

Prepared by

Jeremy C. Phillips[1]
Thierry Menand[1]
R. Stephen J. Sparks[1]
Andrew J. Hogg[1]
John A. Stamatakos[2]
Nancy K. Adams[2]

[1]University of Bristol, Bristol, United Kingdom

[2]Center for Nuclear Waste Regulatory Analyses
San Antonio, Texas USA

May 2008

CONTENTS

FIGURES

ACKNOWLEDGMENTS

This paper was prepared to document work performed by the Center for Nuclear Waste Regulatory Analyses (CNWRA) for the U.S. Nuclear Regulatory Commission (NRC) under Contract No. NRC–02–07–006. The activities reported here were performed on behalf of the NRC Office of Nuclear Material Safety and Safeguards, Division of High-Level Waste Repository Safety. This paper is an independent product of the CNWRA and does not necessarily reflect the view or regulatory position of the NRC. The authors thank Debashis Basu and English Pearcy for technical and programmatic comments, L. Mulverhill for editorial review, and S. Odam for secretarial support.

QUALITY OF DATA, ANALYSES, AND CODE DEVELOPMENT

DATA: Data contained in this report collected at the University of Bristol under a CNWRA contract meet quality assurance requirements described in the CNWRA Quality Assurance Manual. Data and analyses are documented in Scientific Notebooks 88, 555, and 619.

ANALYSES AND CODES: No specialized or controlled software was used in this report.

1 INTRODUCTION

1.1 Background

Volcanic hazards at Yucca Mountain are a concern to the safe disposal of nuclear waste because the potential high-level nuclear waste repository at Yucca Mountain would be located within one of the geologically active volcanic fields in the Great Basin. In the Yucca Mountain region, more than 40 basaltic vents have formed in the past 11 million years. There are 6 cinder cones within 20 km [12.5 mi] of Yucca Mountain that formed in the last million years (e.g., Fleck, et al., 1996). Because of the potential to disrupt the repository and transport radionuclides to the surface, volcanic hazard assessment has been a focus of study since Yucca Mountain was first proposed as a potential repository site. Quantitative estimates of the potential radiological risks that could result from future igneous activity include evaluations of a broad range of models and data proposed by the U.S. Department of Energy (DOE) to support their performance assessment of the repository as required by the regulations in 10 CFR Part 63. A key component of the hazards analysis is to understand how rising basaltic magma would interact with subsurface repository structures, such as tunnels, waste packages, drip shields, and drifts.

To more fully understand potential magma–repository interactions, the Center for Nuclear Waste Regulatory Analyses (CNWRA) tasked researchers at the University of Bristol, Bristol, United Kingdom, to conduct a series of analog experiments. The work was performed on behalf of the U.S. Nuclear Regulatory Commission (NRC) under subcontract to the CNWRA and Southwest Research Institute®. The work was placed at the University of Bristol because of competence in physical volcanology, especially with regard to Dr. S. Sparks, who is recognized throughout the world as a leading expert in volcanology. It is also recognized that the University of Bristol researchers are free of any potential conflict of interest. Work at the University of Bristol under this subcontract has been ongoing since 1998. The work has supported a number of reports and papers (e.g., Basu, et al., 2007; Lejeune, et al., 2002; Menand and Phillips, 2007a,b) as well as inputs to numerous CNWRA and NRC regulatory documents, including Igneous Activity agreement letters, the Integrated Issue Resolution Status Report (NRC, 2005), and the Risk Insights Baseline Report (NRC, 2004).

1.2 Purpose and Scope

This report documents and summarizes important technical aspects of experimental and theoretical work related to sustained magma flow through subsurface structures conducted under the University of Bristol subcontract. Laboratory experiments have investigated the dynamics of how gas-bearing and gas-free fluids similar to magmas that typify basaltic cinder cone eruptions near Yucca Mountain could suddenly decompress, accelerate, and fragment into subsurface openings; convective circulation in magma-filled structures due to gas exsolution and segregation has been investigated. This work is directly linked to the development and verification of numerical models that represent potential decompressive flow processes. Mathematical scaling arguments were developed to describe the subsurface degassing processes and flow patterns, and these showed good agreement with laboratory data. In addition, preliminary laboratory experiments have been conducted to investigate the influence of the viscous drag of recirculating magma flows on small dense particles that represent waste package contents within horizontal drifts.

1.3 Relevance to Staff Review of DOE Information

The work conducted at the University of Bristol as summarized in this report provided staff with information to develop the necessary technical insights into this risk-significant process. Prior to the initial potential consequence work by Woods and Sparks (1998), the DOE work on igneous activity focused mainly on determining the probability of igneous activity, with limited work on the potential consequences to the repository. This focus of activity also reflected the more deterministic and subsystem regulatory requirements in 10 CFR Part 60. With the promulgation of 10 CFR Part 63, the focus shifted to performance-based and risk-informed regulatory requirements. As a result, additional technical support was needed to evaluate the radiological dose consequences of potential igneous activity.

The bases for staff to first develop appropriate conceptual models of magma–repository interactions and then to abstract those concepts into performance assessment models was partially developed from the experimental work at the University of Bristol. This work thereby enabled staff to develop defensible risk insights during the current prelicensing activities with the DOE and address the Igneous Activity Key Technical Agreement items as documented in the Integrated Issue Resolution Status Report (NRC, 2005). Staff anticipate using these results, coupled with other available information on potential igneous activity at Yucca Mountain, to evaluate the DOE license application.

1.4 Report Organization

In addition to the introductory material above, the information provided in this report is organized into three chapters. Chapter 2 consists of three sections and provides an overview of the University of Bristol research into steady-state magma circulation patterns, buoyancy-driven exchange flow between a magmatic dike and a drift, and erosive transport of waste package contents within the drift. Chapter 3 provides the broad implications of the research results for the potential repository. Chapter 4 provides a summary of the important conclusions that can be drawn from the University of Bristol work.

2 STEADY-STATE INTERACTION OF RISING MAGMA WITH A SUBSURFACE DRIFT

2.1 Magma Flow in an Interconnected Dike and Drift

Basaltic volcanism in the Yucca Mountain region is characterized by monogenetic basaltic eruptions, with erupted volumes typically less than 1 km^3 [0.24 mi^3] (Crowe, et al., 1992). Petrological studies suggest that the initial water content of basalts erupted at Yucca Mountain is in the range 1.9–4.6 wt% (Luhr and Housh, 2002; Nicholis and Rutherford, 2004). At typical basalt eruption temperatures of 1,100–1,200 °C [2,012–2,192 °F] and viscosities in the range 10–10^4 Pa s [6.72–6,720 lb_m/ft-s] for this range of compositions, a likely scenario for the interaction of erupting magma with a subsurface drift or tunnel is as follows (Figure 1). The initial interaction is disruption of the drift by the magmatic dike or crack propagating to the surface. This will result in fracturing of the drift internal surfaces and interaction of magma flow with waste packages (e.g., Lejeune, et al., 2002; Woods, et al., 2002). Subsequently, basaltic magma will entirely fill the drift. Because of the shallow depth of subsurface drifts {less than 500 m [1,640 ft] below ground surface} and the high water content of the magma, dissolved water will exsolve as bubbles. Volatile exsolution can increase the liquidus temperature and trigger microlite nucleation, which in turn releases latent heat. This temperature increase might effectively reduce viscosities by a factor of 5–10 compared to the isothermal case (Blundy,

et al., 2006), (i.e., act as a buffer to the viscosity increases caused by decompression exsolution and crystallization), so a starting assumption in this model is that the magma does not experience a significant change in viscosity during emplacement. Initial magma-repository interaction is expected to involve turbulent magma fragmentation but will be followed by the establishment of magma circulation between the dike and the drift due to processes of gas segregation within the drift. As the eruption proceeds, the vertical dike may increase its size and may change from planar cross section to more nearly circular conduit as a result of mechanical and thermal erosion of the host rock.

An important component of the consequence analysis at Yucca Mountain is to understand how rising basaltic magma will interact with subsurface repository tunnels or drifts. The University of Bristol studies have focused on the flow regimes set up by flow in a vertical conduit connected to a horizontal drift, which is a reasonable approximation to the proposed waste repository configuration (Bechtel SAIC Company, LLC, 2004). Experiments have been developed to investigate the potential circulation of bubbly magma within tunnels due to density variations caused by separation of bubbles from the magma. Focusing on conditions of sustained magma flow, a series of laboratory and numerical experiments were conducted to investigate convective circulation in magma-filled structures due to gas exsolution and segregation. The aim of this work was to quantify the time and length scales for bubble segregation and flow recirculation in the drift and the fluxes associated with this gas segregation. For simplicity, the University of Bristol work focused specifically on gas segregation processes without accounting for the presence of waste packages. Also, the Reynolds number (the balance of inertial to viscous forces) in these experiments was estimated to be of order one or less, such that exchange flow of magma within drifts will be essentially laminar.

2.1.1 Low Volumetric Gas Fractions

The initial water content of basalts erupted at Yucca Mountain has been measured to lie in the range 1.9–4.6 wt% (Luhr and Housh, 2002; Nicholis and Rutherford, 2004). Provided that no gas loss from the system has occurred during magma ascent, this range of water content would correspond to volumetric gas fractions between 70 and 90 percent and have magmatic viscosities ranging between 250 and 1,000 Pa s [168 and 672 lb_m/ft-s] (Giordano and Dingwell, 2003; Shaw, 1972). These estimates are based on an average repository depth of 300 m [984 ft] with a 7 MPa [70 bar] lithostatic pressure and an average rock density of 2,400 kg/m^3 [149.8 lb/ft^3] (Bechtel SAIC Company, LLC, 2004). Assuming a basalt solubility of 3×10^{-6} $Pa^{1/2}$ (Woods and Huppert, 2003) and an initial water content of 4.6 wt% water, the amount X of exsolved water is 3.8 wt% at the depth of the repository. The density of water vapor, ρ_g, is 12.2 kg/m^3 [0.0004 lb/in^3] if exsolved water vapor follows the perfect gas law and the temperature of magma is 1,273 K [1,830 °F]. Using the following equation (Menand, et al., 2007), the volumetric gas fraction (c) is obtained from the exsolved mass fraction (X):

$$\frac{(1-c)}{c} = \frac{\rho_g}{\rho_l}\frac{(1-X)}{X} \qquad (1)$$

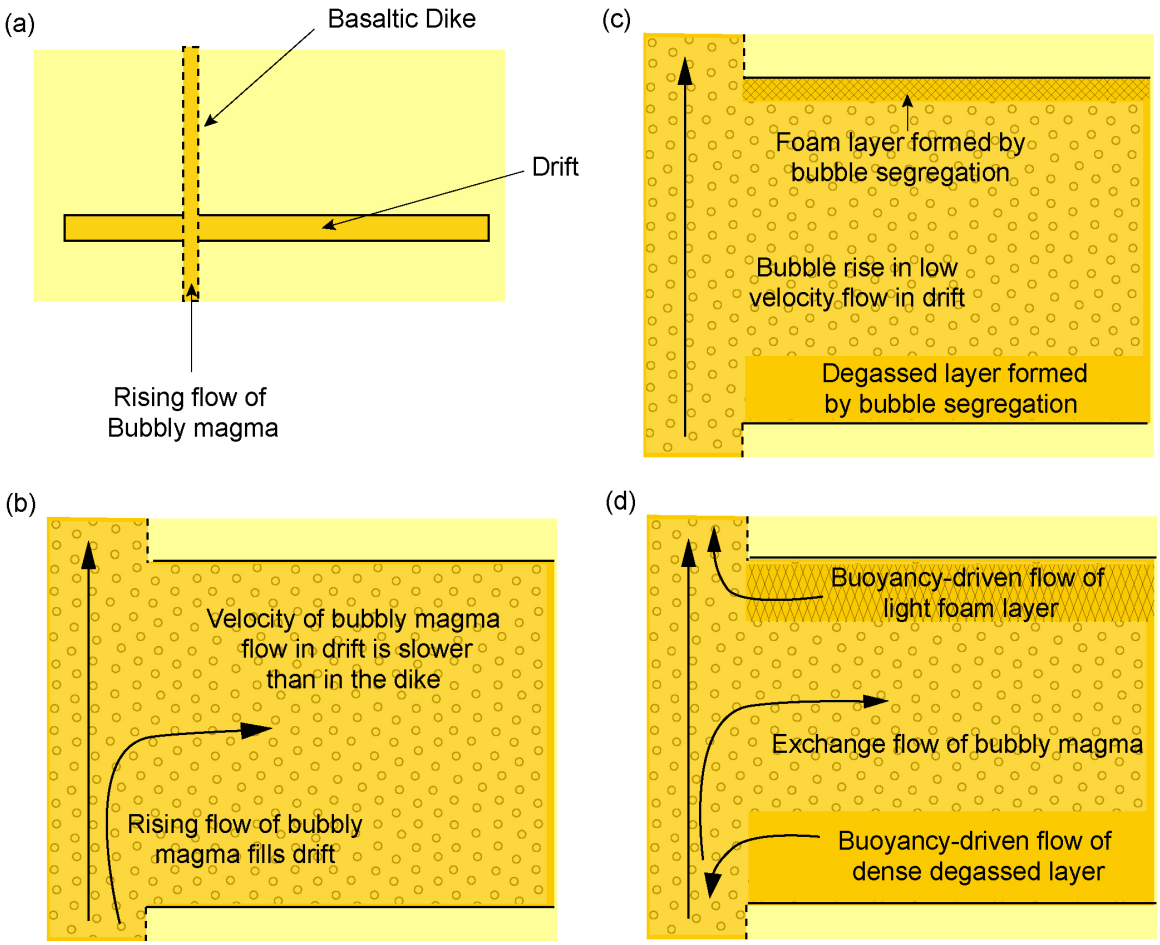

Figure 1. Schematic Diagram of Magma Flow in an Interconnecting Dike and Drift: (a) System Geometry, (b) Initial Condition With the Drift Filled With Bubbly Magma From the Dike, (c) Bubble Segregation Within Drift, and (d) Steady-State Exchange Flows Set Up by Bubble Segregation.

For a magma density (ρ_l) of 2,750 kg/m^3 [171.7 lb/ft^3] (Lange, 1994), this expression gives a volumetric gas fraction c = 0.9. We note, however, that such a volumetric gas fraction is much higher than the generally accepted value of 0.7 for generic foams (Cashman, et al., 2000; Jaupart and Vergniolle, 1989; Sparks, 1978). Given that it is not clear whether gas loss will occur deeper in the system, these high gas fractions (0.7–0.9) are regarded as representing the upper endmember of a wide range of gas contents, which are investigated here.

Initial experiments focused on the case of low volumetric gas fraction (<10 percent) in which the flow dynamics are not influenced by bubble–bubble interactions. A low volumetric gas fraction is also of interest for the waning stage of a basaltic eruption, which is characterized by effusive flow of degassed magma (Vergniolle and Jaupart, 1990). This case enables identification of gas segregation processes that can occur within a magma-filled drift and quantification of how these processes can affect flow circulation within that drift.

Gas segregation in a magma-filled drift intersected by a vertical dike was investigated using analog experiments with two interconnected glass tubes; both ends of the vertical glass tube were connected to a peristaltic pump to form a recirculating flow loop (Figure 2). Degassing involving low volumetric gas fractions (<10 percent) was simulated by electrolysis, producing micrometric bubbles in viscous mixtures of water and golden syrup. The Reynolds number in the experiments ranged from 0.1 to 3.

The presence of exsolved bubbles induces a buoyancy-driven exchange flow between the dike and the drift, in which bubbly fluid flows from the dike into the drift as a viscous gravity current (Figure 3a). This exchange flow is slow enough that bubbles in the drift have time to rise, segregate from the fluid, and accumulate as foam at the top in conjunction with the accumulation of degassed fluid at the base of the drift (Figure 3b). Ultimately a steady state is reached whereby influx of bubbly fluid into the drift is balanced by outward flux of lighter foam and denser degassed fluid back into the dike (Figure 3c). The length scale of the intrusion of bubbly fluid into the drift and the time scale of the gas segregation that occurs there are both controlled by the rise of bubbles within the drift. The results of this work have been applied to gas segregation in the plumbing systems of basaltic volcanoes and have been published in the Journal of Volcanology and Geothermal Research (Menand and Phillips, 2007a).

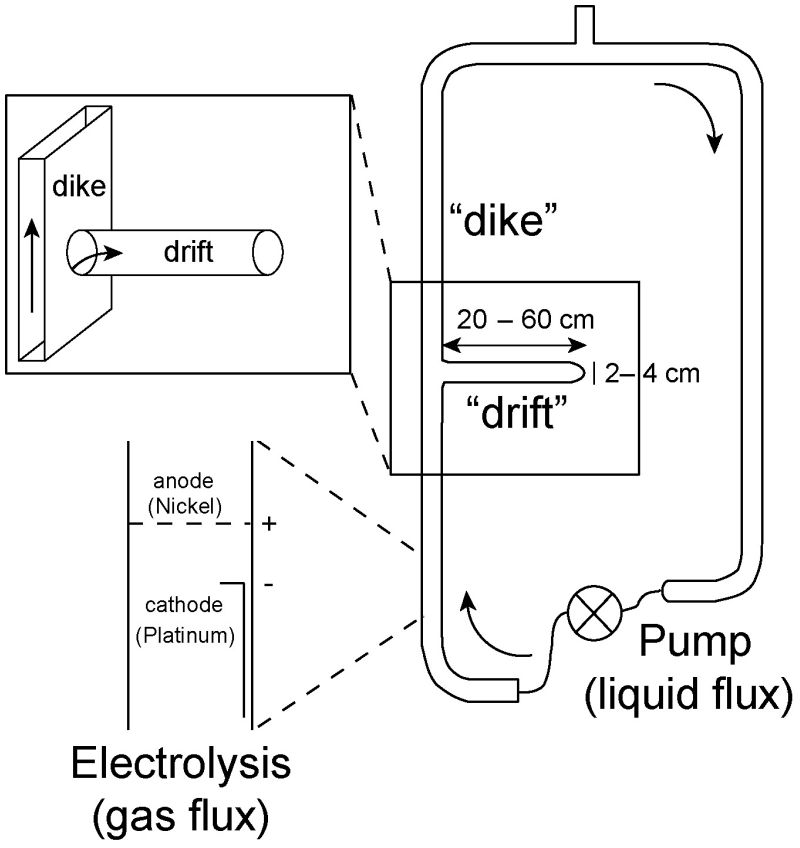

Figure 2. Schematic Diagram of the Experimental Apparatus

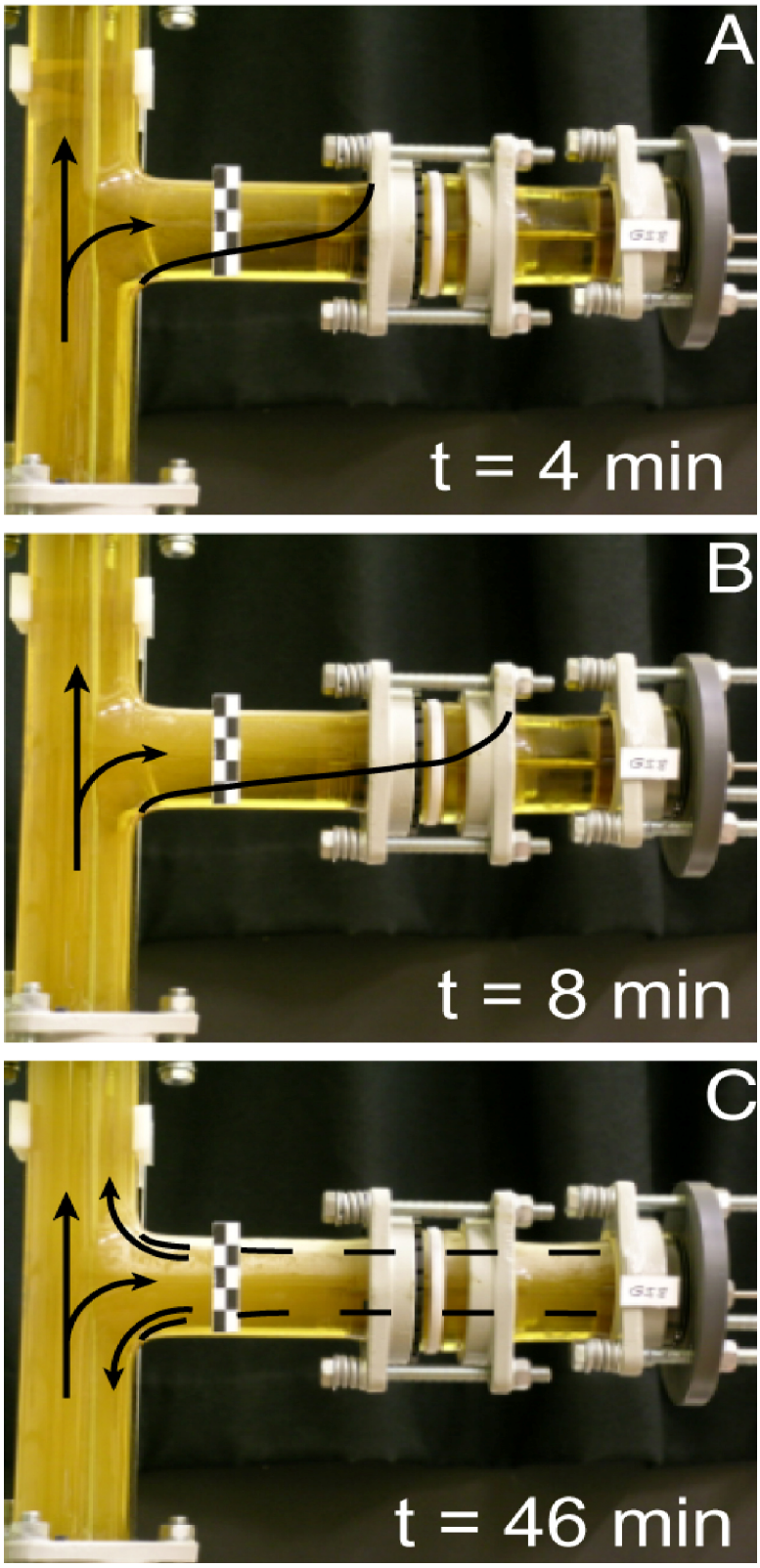

Figure 3. Establishment of a Steady-State Exchange Flow Between a Vertical Tube and a Horizontal Side Arm

2.1.2 High Volumetric Gas Fractions

The high volumetric gas fractions of 70 to 90 percent expected at the shallow depth of the Yucca Mountain repository correspond to values that are as high as or even higher than values generally accepted as typical for generic foams (Vergniolle and Jaupart, 1990). Based on examples such as Stromboli Volcano in Italy, magmas interacting with the potential Yucca Mountain repository might be expected to display an explosive behavior characterized by repeated coalescence and collapse of the foam (Vergniolle and Jaupart, 1990). The higher bubbly gas fraction in the rising magma may also lead to competing effects in the exchange flow between dike and drift. The density contrast between the degassed magma in the drift and the bubbly magma rising in the dike would increase if the rising magma has a higher gas content, but the density contrast between the bubbly magma in the drift and the overlying foam layer would decrease. In addition, a higher gas fraction would increase the viscosity of the intruding bubbly magma.

To better understand how high volumetric gas fractions would affect any exchange flow between a dike and a drift and how bubbly collapse would interact with convective circulation in magma-filled drifts, additional laboratory experiments were carried out with mixtures of water and golden syrup that are aerated before being injected into the recirculating flow loop. The aeration technique leads to volumetric gas fractions as high as 40 percent. Collapse of the bubbly mixture was simulated by the separate injection of gas slugs within the flow loop during the experiments. Gas slugs were injected either within the drift or below the dike–drift junction to simulate foam collapses occurring either within the drift or within the dike. The laboratory experiments showed that the same processes occurred as for lower volumetric gas fractions, with the increased viscosity and reduced density contrast increasing the time scale for gas segregation as suggested above. The results of this work have been submitted to the Journal of Volcanology and Geothermal Research (Menand and Phillips, 2007b).

If these results are scaled up to the Yucca Mountain repository, steady-state gas segregation could be accomplished before magma temperatures cool below the solidus depending on the viscosity of the degassed magma, the rate of cooling of the magma, and the average size of exsolved gas bubbles. The fluxes associated with gas segregation range from 1 m^3/s [35.3 ft^3/s] for the less viscous magmas to 0.01 cm^3/s [6.1×10^{-4} in^3/s] for the most viscous degassed magmas, with associated velocities ranging from 0.1 m/s to 10^{-9} m/s [0.32 to 3.2×10^{-9} ft/s] for the same viscosity range. Also, the Yucca Mountain system is likely to be in an unstable foam collapse regime, with the foam accumulated by gas segregation at the top of the drift reaching only a few centimeters in thickness before its collapse by bubble coalescence (Jaupart and Vergniolle, 1989; Menand and Phillips, 2007a). The relative proportion of erupted degassed magma, which might potentially carry and entrain nuclear waste material toward the surface, would depend on the value of the dike magma supply rate relative to the value of the gas segregation flux. Violent eruption of gas-rich as well as degassed magmas would occur at relatively high magma supply rates, and eruption of mainly degassed magma by milder episodic Strombolian explosions would occur at relatively lower supply rates. Depending on the average size of exsolved gas bubbles, the critical magma supply rate that delimits these two eruptive regimes would range from 10^{-4} to 1 m^3/s [3.5×10^{-3} to 35.3 ft^3/s] for a magma viscosity of approximately 10 Pa s [6.72 lb_m/ft-s] and 10^{-8} to 10^{-4} m^3/s [3.5×10^{-7} to 3.5×10^{-3} ft^3/s] for a magma viscosity of approximately 10^5 Pa s [6.72×10^4 lb_m/ft-s].

2.1.3 No Gas

Although magmas erupting at Yucca Mountain would likely contain nonnegligible amounts of volatiles and thus be vesiculated at the depth of the proposed repository, the convective

circulation of bubble-free magma within a drift intersected by a dike was investigated. As in the case of low volumetric gas fractions, this scenario is of interest for the waning stage of a basaltic eruption, which is characterized by effusive flow of degassed magma (Vergniolle and Jaupart, 1990). Considering a drift with a closed end, the flow dynamics are entirely controlled by the solid boundaries, leading to development of driven cavity flow, in response to the vertical movement of magma up the dike. This flow is characterized by the development of a succession of counterrotating vortices in the drift (Shankar and Deshpande, 2000). In laboratory experiments using bubbly viscous liquids (as previously discussed in Sections 2.1.1 and 2.1.2) the development of a succession of vortices was not observed, suggesting that the buoyancy-driven flow due to gas segregation dominated any control on the flow by the boundaries. When a separate gas phase has exsolved, a single vortex is observed at the dike–drift junction.

The geometry of a dike intersecting a drift at the Yucca Mountain repository corresponds to a cavity of very large length:width aspect ratio, which can thus be considered as infinite. In this case, previous studies found that the size of the primary vortex that is closest to the conduit/dike increases proportionally with the square root of the Reynolds number of the flow in the conduit (Shankar and Deshpande, 2000). These studies found also that the strength of the vortices is proportional to the Reynolds number of the flow in the conduit and decreases away from the conduit (Figure 4). This means that the primary vortex, closest to the entrance of the cavity, is always the strongest. Comparing the downward velocity scale of the primary vortex, which is the highest vertical velocity scale induced by vortices, with the upward rise velocity of the bubbles in suspension provides a reason why no vortices were observed in the bubbly experiments. Vortices would develop and control the structure of the flow if their velocity scale is larger than that of the rising bubbles. For conditions similar to those explored in the analog experiments with low volumetric gas fractions, this is the case for the first vortex only. Additional vortices further away from the conduit cannot develop vertical velocity scales greater than the rise speed of the segregating bubbles and are thus not observed.

2.2 The Dynamics of Viscous Displacement Flows

In Section 2.1.3, the development of vortices in bubble-free viscous liquids representing magma circulating within a drift intersected by a dike was considered. Minus the effects of bubbles, the flow dynamics are controlled by the solid boundaries. However, the effect of both an upper and lower solid boundary is not adequately described in previous studies; new analysis of buoyancy-driven exchange flow between two viscous liquids is required. Here, the density-driven displacement of one fluid by another within a horizontal, two-dimensional channel was analyzed. The configuration for the analysis is shown in Figure 5 and consists of fluids with densities (ρ and $\rho-\Delta\rho$) and viscosities ($\mu 1$ and $\mu 2$), separated by an interface at position $z = h(x,t)$ within a channel of height d, where the coordinate axes are aligned so that x is horizontal and z is vertical. The analysis examined the evolution of the interface $h(x,t)$ as the fluids displace one another, driven by gravitational forces associated with the difference in density between them.

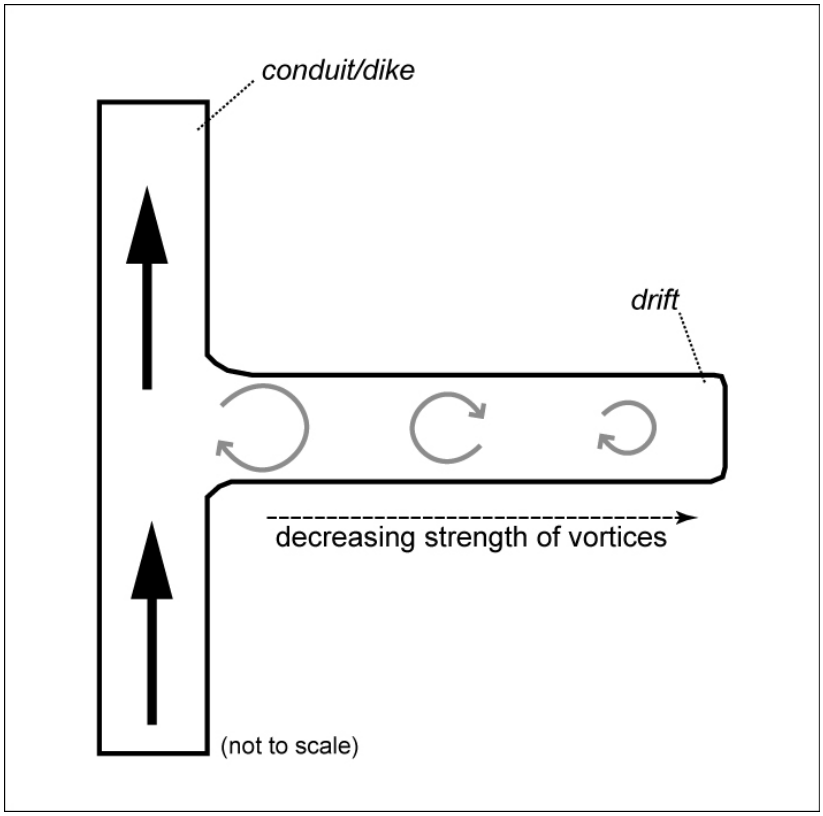

Figure 4. Development of Vortices (Gray Arrows) in a Drift Connected to a Vertical Conduit (Black Arrows Indicate Vertical Flow)

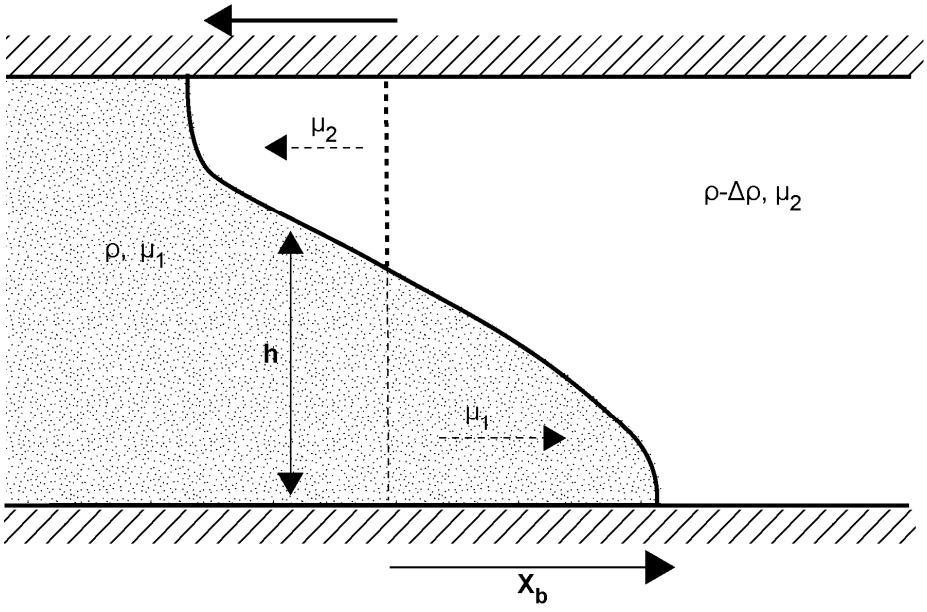

Figure 5. The Configuration of the Flow

Assuming the horizontal length scale for the motion far exceeds the vertical length scale, the motion is predominantly horizontal. This implies that the pressure distribution, p, is hydrostatic and that its gradient is given by

$$\frac{\partial p}{\partial x} = \begin{cases} \frac{\partial p_T}{\partial x} + \Delta\rho g \frac{\partial h}{\partial x}, & 0 < z < h \\ \frac{\partial p_T}{\partial x}, & h < z < d \end{cases} \qquad 2$$

where $pT(x)$ is an, as yet, unknown pressure along the upper boundary of the channel, and g denotes gravitational acceleration. Next, based on the assumptions (i) that the Reynolds number of the motion, $Re = \rho UL/\mu$, where U and L are representative velocity and horizontal length scales, respectively, is of order unity; (ii) that the surface tension on the interface is negligible; and (iii) that chemical diffusion of the dissolved species causing the density difference is also negligible, the dynamics are seemingly controlled by a balance between the divergence of viscous stresses and the pressure gradient within each layer. Thus

$$\mu_1 \frac{\partial^2 u_1}{\partial z^2} = \frac{\partial p_T}{\partial x} + \Delta\rho g \frac{\partial h}{\partial x} \qquad 3$$

and

$$\mu_2 \frac{\partial^2 u_2}{\partial z^2} = \frac{\partial p_T}{\partial x} \qquad 4$$

Furthermore, the interface is merely advected as a kinematic boundary, and there can be no net mass flux within the channel. These conditions, together with the flow boundary conditions of no slip at the upper and lower channel boundaries and continuity of velocity and shear stress at the interface, allow the derivation of the following evolution equation for the interface between the fluids.

$$\frac{\partial h}{\partial t} = \frac{\Delta\rho g}{3\mu_1} \frac{\partial}{\partial x}\left(h^3 (d-h)^3 \frac{d-(1-r)h}{(1-r)(d-h)^4 - rh^4 + rd^4} \frac{\partial h}{\partial x} \right) \qquad 5$$

where $r = \mu_2/\mu_1$.

Simple scaling can be used to relate the rate of propagation to the material properties of the flow. This relationship will underlie a similarity solution (constructed below), and it clearly reveals the interplay of the dynamical effects. The streamwise pressure gradient is estimated by $\partial p/\partial x \sim \Delta\rho g d/L$, where the interface height scales with the channel height, d. If the divergence of the viscous stresses is $\sim \mu u/d^2$, and u is identified as $\sim L/t$, a connection between horizontal length scales and time can be noted $L \sim (\Delta\rho g d^3 t/\mu)^{1/2}$. This yields a similarity solution to Eq. (5) of the form

$$h(x,t) = dH(\eta) \qquad 6$$

where

$$\eta = \frac{x}{\left[\Delta\rho g d^3 t/\mu_1\right]^{1/2}} \qquad 7$$

Substitution in the governing equation reveals that the sole remaining dimensionless quantity is the ratio of the viscosities $r = \mu_2/\mu_1$. In particular, the foremost points at which the two fluids have intruded into each other at the upper and lower boundaries are given by

$$x_t(t) = \eta_t(r)\left(\Delta\rho g d^3 t/\mu_1\right)^{1/2} \qquad 8$$

and

$$x_b(t) = \eta_b(r)\left(\Delta\rho g d^3 t/\mu_1\right)^{1/2} \qquad 9$$

where η_t and η_b, functions only of the viscosity ratio, r, are to be determined as part of the solution.

The equation governing the similarity solution numerically can be integrated to find interface profiles that depend upon r. Two examples are shown in Figure 6a; when $r = 1$, the interface is symmetric about the midpoint. When $r \neq 1$, however, this symmetry is lost, and the less viscous fluid intrudes further, albeit with a shallower interface. The variation of the position of the upper and lower interface positions with the viscosity ratio is also plotted in Figure 6b. The numerically calculated positions are shown alongside an asymptotic calculation valid when $r \ll 1$.
In particular

$$\eta_t^2 + 4\log\eta_t = -6.8792 - \tfrac{4}{3}\log(r) \qquad 10$$

and

$$\eta_b = 0.4924 \qquad 11$$

Note that in Figure 6b, only curves for $r<1$ are plotted. This is because for values of r in excess of unity, it is straightforward to calculate the appropriate profiles by a simple rescaling of the results for $1/r$.

Simple laboratory experiments have been performed to validate this theory by removing a vertical barrier between two viscous fluids of differing densities and viscosities within a horizontal, Perspex channel. The medium used is a golden syrup, diluted to alter its viscosity, in which salt was dissolved to vary the density. In Figure 7, a photograph of an experiment is shown in which the less dense solution has been dyed red to aide visualization.

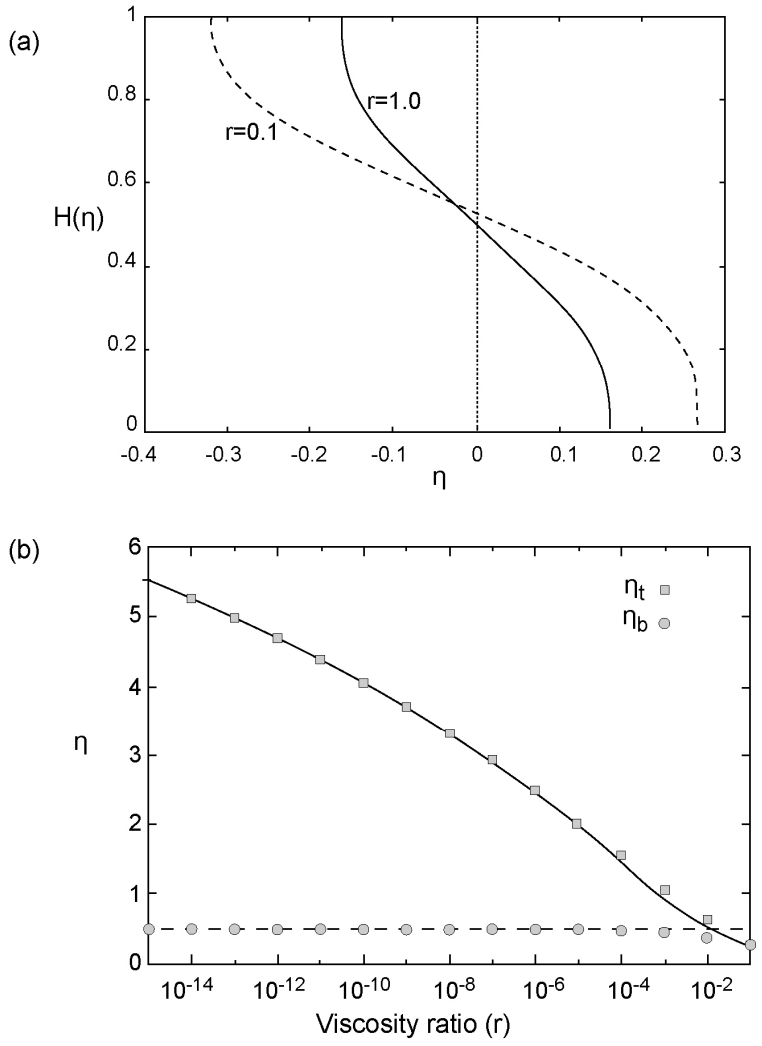

Figure 6. (a) The Self-Similar Shape of the Interface, H(η), at *r* = 1 and *r* = 0.1. (b) The Self-Similar Positions of the Interface at the Upper and Lower Boundary as a Function of the Viscosity Ratio, *r*. Both Numerical (Symbols) and Asymptotic Values (Lines) Are Plotted.

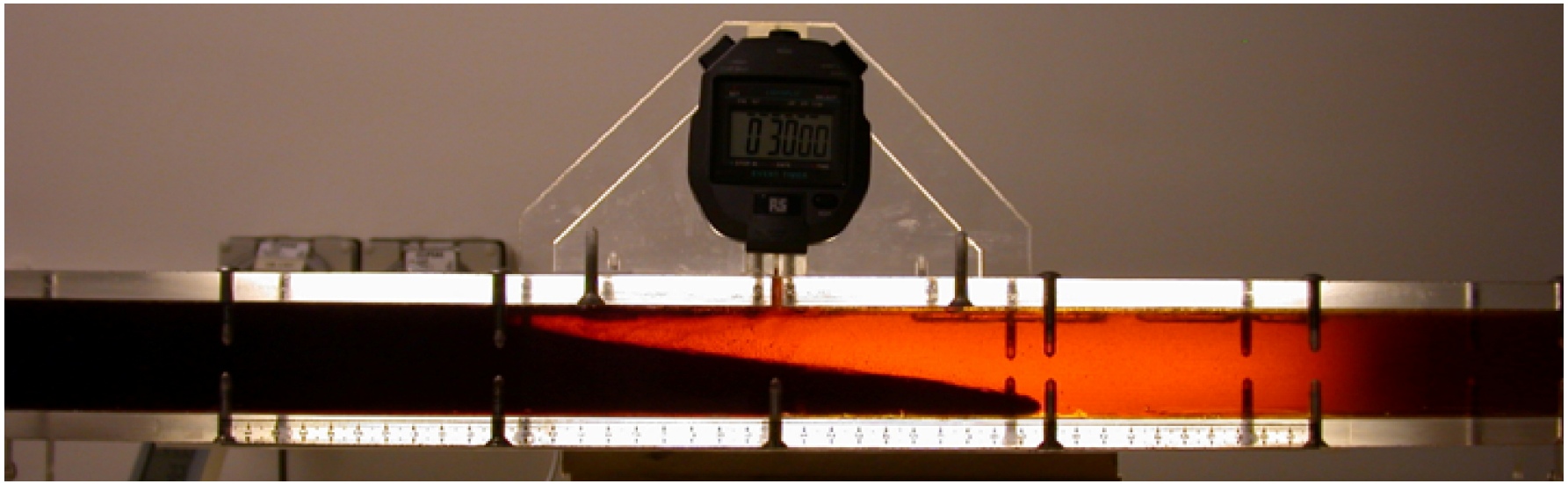

Figure 7. Photograph of the Laboratory Experiment 30 Minutes After the Flow Was Initiated. In This Experimental Run, the Viscosities of the Two Fluids Are Equal.

The ensuing motion was recorded and used to determine the evolution of the interface between the two solutions. By performing a series of experiments at a range of density differences and viscosity ratios, the rate at which x_t and x_b evolve and their dependency upon the viscosity ratio was observed. In Figure 8a, the positions of the fronts on the upper and lower boundaries are shown to vary with $t^{1/2}$, as predicted by theory. Furthermore, there is close agreement between the experimentally determined and theoretically predicted coefficients of proportionality, η_t and η_b. In Figure 8, the experimentally measured interface profile at various times during an experimental run are plotted. Figure 8 shows that the interface adopts a self-similar profile that may be accurately predicted by the model.

2.3 Erosive Transport of Dense Bodies in Viscous Shear Flow

An important consequence of magma flow between an intersecting dike and drift is the potential transport of waste material from the drift to the dike and possibly to the surface via an eruption. Magma flow may be generated by density differences between bubble-rich and bubble-poor magma (described previously in Sections 2.1.1 and 2.1.2) or by viscous coupling of the rising dike flow with magma present in the drift (described previously in Section 2.1.3). Erosive transport of small particles by turbulent stream flows has been widely studied in sedimentology, and the key parametric relationship between the Shields number θ (ratio of shear stress acting on a particle to its weight) and particle diameter (taking into account the effect of inertial and viscous forces of the flow) has been empirically determined for turbulent flow conditions (Leeder, 1999). However, the parametric dependence and key controls on particle motion have not been determined for the case of a viscous shearing flow, such as magma flow. Preliminary experimental and theoretical investigation of the transport of small particles (analogous to waste package contents in pelletal form) in a viscous shearing flow is described below.

Laboratory experiments were conducted to study the erosive transport of small dense bodies by unidirectional viscous flows in a cylindrical pipe, shown schematically in Figure 9. The pipe diameter was 4 cm [1.57 in], and the viscous fluid was a mixture of water and golden syrup (sugar syrup) with densities in the range 1,200 to 1,260 kg/m^3 [74.91 to 78.66 lb/ft^3], and viscosities in the range 0.06 to 1.5 Pa s [0.04 to 1.00 lb$_m$/ft-s]. The dense bodies were elongate cylinders of approximately 3 mm [0.1 in] diameter and 5 mm [0.2 in] long, with a density of 3,100 kg/m^3 [193.5 lb/ft^3]. The fractional height of the pipe occupied by the dense bodies was about 0.08, and the viscous liquid volumetric flow rate ranged up to 30 cm^3/s [0.94 ft^3/s]. The critical Shields number relationship for these flows is shown in Figure 10a, with the parametric dependence for turbulent flow shown in Figure 10b for comparison. These preliminary experiments were not further developed due to the publication of similar results and associated theoretical interpretation (Charru, et al., 2004).

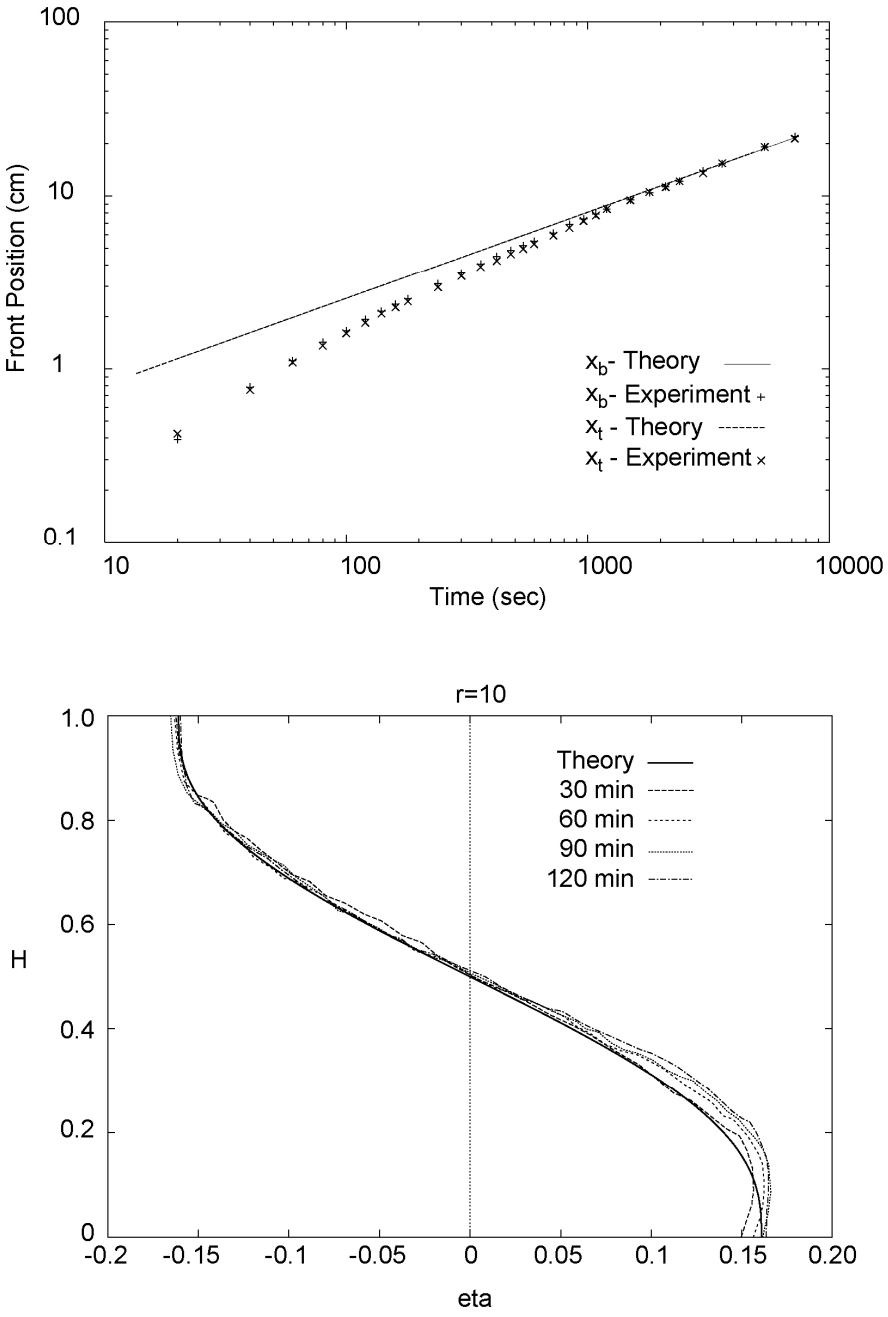

Figure 8. (a) The Position of the Interface Between the Two Fluids on the Upper and Lower Boundaries as a Function of Time. Also Plotted Is the Theoretical Prediction. Note That Because the Viscosities Are Equal (*r* = 1), the Two Positions Should Increase at the Same Rate. (b) The Profile of the Interface at Various Times During an Experiment Plotted Against the Similarity Variable *H*. This Confirms That the Flow Evolves Into a Self-Similar State.

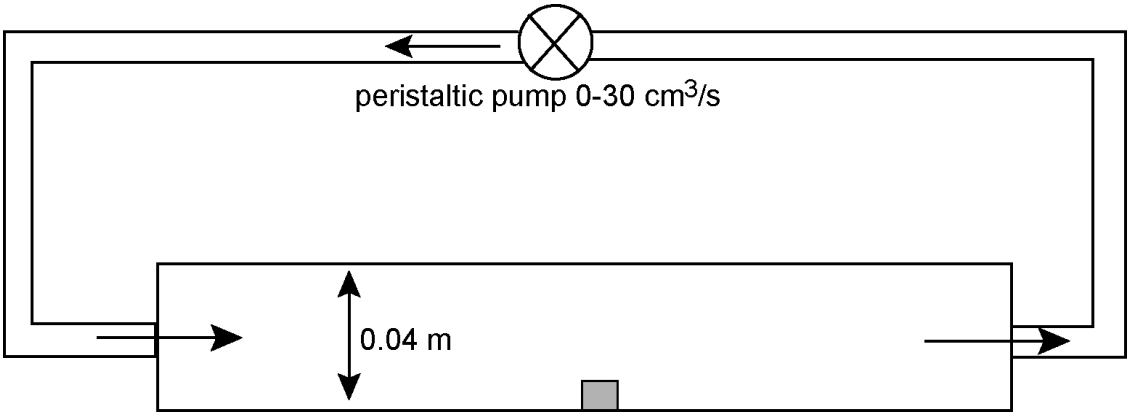

Figure 9. Schematic Diagram of the Flow Loop Used for Erosive Viscous Flow Experiments

The experimental and theoretical studies of Charru, et al. (2004) provide a framework for estimating the transport properties of small particles in a uniformly sheared viscous flow. Experiments were conducted in a rotating annular viscous flow to achieve steady flow over long times and under conditions in which the secondary velocity generated by centrifugal forces was negligible compared to plane Couette flow in the channel. They showed similar critical Shields number dependence to our experiments (Figure 10a) and that small particle motion took the form of a series of saltation "flights," whose duration τ was found to be independent of shear rate, γ,

$$\tau \approx 15 d / v_s \qquad 12$$

where d is the particle diameter, and v_s is the Stokes settling speed of the particle. The mean particle velocity, $\overline{u}$, was found to depend linearly on shear rate

$$\overline{u} \approx 0.1 \gamma d \qquad 13$$

The particle flow rate, Q_p, was found to have a quadratic dependence on shear rate

$$Q_p \approx 0.1 \gamma (0.47 / d)(\theta - 0.12) \qquad 14$$

Erosive transport of small particles by fluid flow is a complex process that depends on interaction of the particles and fluid and the particles with each other. Further work is required to understand the flow conditions representative of potential magma-waste repository interaction and particle transport under these conditions. However, the scaling arguments presented here form a fundamental framework for estimating potential transport properties of high density particles such as small fragments of spent nuclear fuel in a viscous magma return flow. This can be illustrated with simple estimates for magma properties for basalt in the Yucca Mountain region {density of 2,750 kg/m^3 [171.7 lb/ft^3], viscosity of 10 Pa s [6.72 lb$_m$/ft-s], 70 vol% of degassed bubbles 1 mm [0.04 in] in diameter}, assuming that the magma flow pattern corresponds to flow through a circular cross-section drift, (i.e., a standard Poiseuille flow profile

for viscous flow in a cylindrical cross-section [Schlichting, 1960]). The presence of waste containers or debris on the floor of the drift will complicate the flow patterns (e.g., create local eddies that can affect Couette flow dynamics), but the principles illustrated here should hold. For a maximum average velocity of degassed magma in a 5-m-diameter [16.4 ft] and 1-km-long drift [0.6 mi] of about 10^{-3} m/s [0.003 ft/s] (using equation 17 in Menand, et al. [2007] for the flux), the maximum shear rate 0.1 m [0.3 ft] above the base of the drift is approximately 7.5 s^{-1}. Using a particle size range of 10 to 500 microns [3.9×10^{-4} to 0.02 in] (CRWMS M&O, 2000) for spent nuclear fuel that has been fragmented by disruptive processes with a density of 10,000 kg/m^3 [624.3 lb/ft^3], the maximum Shields number is about 2 for this viscous flow (Charru, et al., 2004), corresponding to a particle flow rate of about 1,500 particles per unit drift width per second (Eq. 14). This particle flow rate is estimated for the largest fragments of spent nuclear fuel 500 microns [0.02 in] in diameter. Particle transport from potentially disrupted waste containers will be limited by the volume of particles available to the flow, the cooling times of the magma, and the effects of surface roughness for the very complex geometries of a disrupted waste package containing high level waste.

3 IMPLICATIONS FOR POTENTIAL MAGMA–REPOSITORY INTERACTIONS AT YUCCA MOUNTAIN

These studies have focused on the flow regimes set up by flow in a vertical conduit connected to a horizontal drift, which abstracts the geometry of potential magma-drift interactions at Yucca Mountain (Bechtel SAIC Company, LLC, 2004). At the relatively shallow depths of the drifts and tunnels, most of the volatile content of the ascending basalt is expected to exists as exsolved bubbles (~3.8 wt% out of 4.6 wt%) ranging in diameter between 0.1 and 1.0 mm [0.004 and 0.04 in] (Cashman and Mangan, 1994; Sarda and Graham, 1990; Sparks, 2003). This percentage of exsolved bubbles assumes that the magma pressure is lithostatic, the true magma pressure will depend on the eruption dynamics. There may be a range of bubble volumetric contents depending on the amount of gas loss at depths greater than the potential repository as the magma ascends. Also, the amount of exsolution depends not only on the magma rise dynamics but also the geometry of the deeper plumbing system; horizontal elements such as sills can act as extremely efficient gas segregators (Menand and Phillips, 2007a,b). The amount of exsolved gas present in magma within the drift is critical because this determines the nature and strength of potential magma circulation in the drift.

In the unlikely case that all the exsolved bubbles have segregated from the magma by the time magma reaches the repository depth (i.e., the no gas case discussed in Section 2.1.3), circulation of magma potentially filling the drift can occur, driven by viscous coupling with the rising magma in the connected dike. This viscous coupling leads to the formation of a series of counterrotating vortices within the drift. Studies suggest that the characteristic velocity of the vortices within the drift decreases rapidly with distance away from the intersection with the vertical conduit. These vortices are not observed when bubbles are present because the rise speed of the bubbles is greater than the vertical velocity scales of the vortices. Thus, in the case of bubble-free magma, the velocity of magma circulation within the drift is low compared to bubbly magma buoyancy-driven flow, and only very small drag forces are exerted on the contents of the drift. Also, lower circulation velocities could decrease the time taken for magma to solidify.

(a)

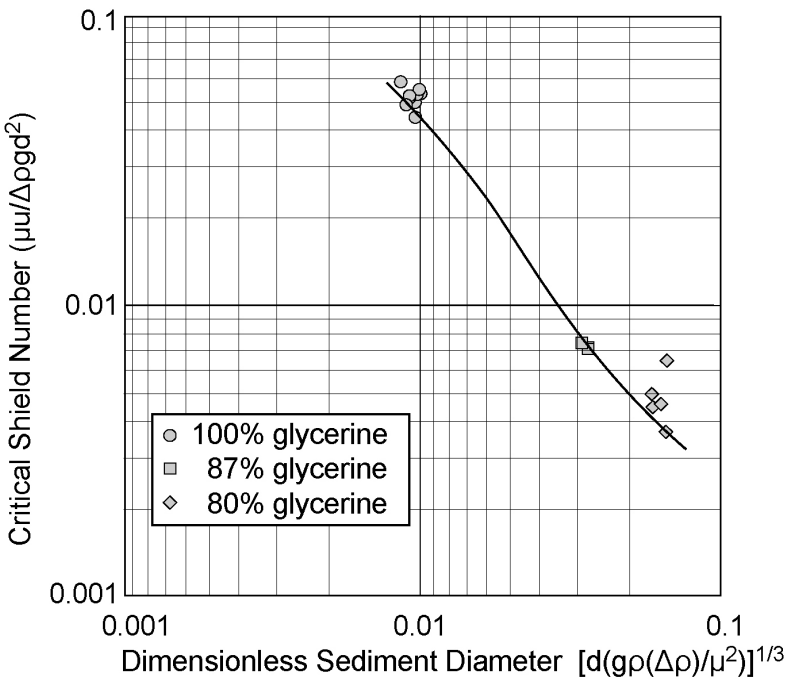

(b)

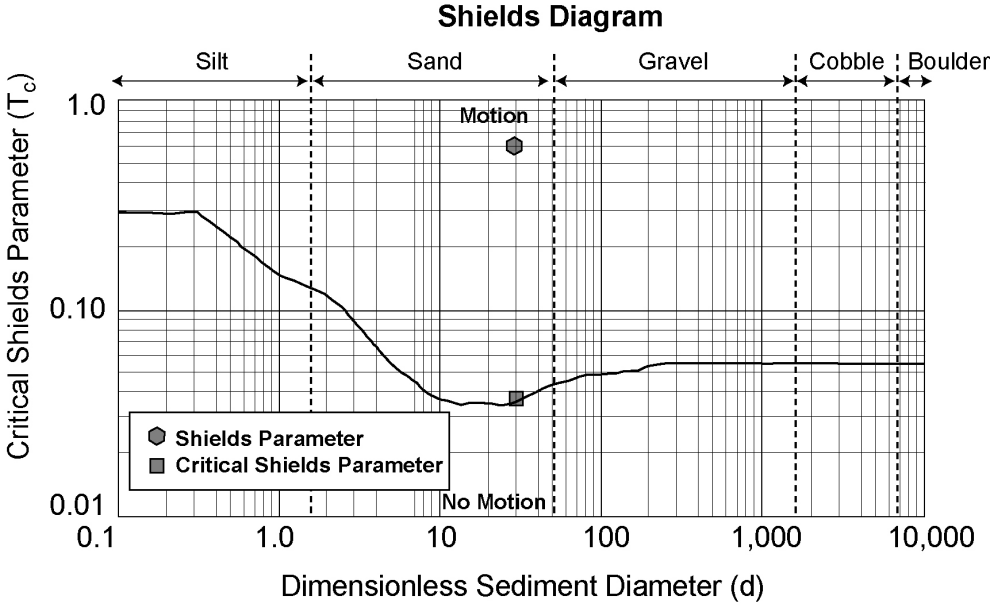

Figure 10. The Relationship Between Critical Shields Number and Sediment Diameter for (a) Small Dense Bodies in Viscous Pipe Flow and (b) Dense Particles in Turbulent Stream Flow

The relatively high volatile content measured for Yucca Mountain basalts (Nicholis and Rutherford, 2004) suggests that future eruptions will most likely produce flows of bubbly magma at the depth of the potential waste repository. Initial disruption of a drift by bubbly magma containing the highest estimates of volatile content reported by Nicholis and Rutherford (2004) would presumably be turbulent and involve magma fragmentation. At the lower end of the dissolved volatile range, however, the dynamics of unfragmented magma circulation between conduit and drift will be controlled by the dynamics of bubble segregation within the drift. Bubbles are able to rise and segregate from the magma in the horizontal drift, forming a gas-rich foam at its top, and the residual degassed magma is more dense than the bubbly magma in the vertical conduit, so a buoyancy-driven exchange flow is set up (Figure 1). The characteristic velocity of this exchange flow is much greater than any vortical circulation generated by viscous coupling with the vertical flow in the conduit and therefore dominates. At a distance greater than 15–20 m [49–66 ft] from the dike intersection, the characteristic vortical velocity is smaller than 10^{-10} m/s [3.28×10^{-10}ft/s] and thus slower than the velocity at which bubbles rise through the magma. Analysis of the dynamics of buoyancy-driven exchange flow with upper and lower solid boundaries shows that for bubble sizes of 0.1 to 1 mm [0.004 to 0.04 in], the buoyancy-driven exchange flow may occupy the full length of a 500 m [1,640 ft] drift. Steady-state magma circulation could be established within the drift on time scales that can be as short as a few days based on magma viscosities of 100 to 1,000 Pa s [67.2 to 672 lb_m/ft-s]. For comparison, NRC (1999) estimated that it would take approximately 30 days for temperatures in a 5-m [16.4-ft]-diameter magma-filled drift to drop below 1,000 °C. This 30-day estimate is a minimum because it assumes conductive cooling of the magma in the drift without considering the circulation and replenishment of the drift with hotter magma as the eruption proceeds or the latent heat of crystallization.

The fluxes of recirculating magma will depend on the depth of the foam layer formed by segregating bubbles at the top of the drift and the magma flux supplied to the drift by the eruption. The eruptive magma flux for previous basaltic volcanic activity at Yucca Mountain is not well constrained but will probably fall within typical values for monogenetic basaltic eruptions of 1 to 10 m^3/s [353 ft^3/s] (Duffield, et al., 1982). The foam layer depth in the basalt magma in the drift containing 3.8 wt% exsolved water is estimated at approximately 0.6 m [2.0 ft] for bubbles 0.1 mm [0.004 in] in diameter. This foam layer depth decreases to approximately 0.06 m [0.20 ft] for bubbles 1 mm [0.04 in] in diameter. Because these values of foam thickness and bubble size exceed critical values for magmatic foam collapse calculated using the method of Jaupart and Vergniolle (1989), steady-state degassing is predicted to occur via periodic foam collapse. For foam layers of these depths, the model described previously suggests steady-state exchange fluxes of bubbly and degassed magma between the vertical conduit and horizontal drift in the range of 10^{-2} to 10^{-6} m^3/s [0.35 to $3.5 \times 10^{-5}$$ft^3$/s]. Furthermore, first order estimates indicate that exchange flows of degassed magma have the potential to transport small fragments of spent nuclear fuel toward the active vertical conduit and thus to the surface via the eruption. However, these are only first order estimates. Viscous flow around undisturbed waste packages and drip shields could lead to a more complex flow and lower fluxes, which may not support waste entrainment.

Qualitative observations from these laboratory analog experiments suggest that the dynamics of gas segregation in a drift will be independent of the magma supply rate in the vertical conduit for magma supply fluxes in the range 0.1 to 100 times that of the exchange flow flux in the drift (Menand and Phillips, 2007a). The foam collapse regime that is likely for an eruption at the Yucca Mountain site could lead to episodic Strombolian activity due to periodic release of collapsing foam. This episodic Strombolian activity may lead to further explosive enlarging of the vertical conduit, thereby promoting an increase in the magma supply rate. Experimental results from the work conducted at the University of Bristol indicate a critical magma supply rate

of between 10^{-2} and 10^{-6} m^3/s [0.35 and 3.5×10^{-5} ft^3/s] for the transition between the foam collapse regime and a more explosive regime in which bubbly magma supplied from depth is erupted before significant gas segregation can take place (Menand and Phillips, 2007a).

4 CONCLUSIONS

In a series of experimental and numerical analyses, sustained magma flow through subsurface structures was investigated to more fully understand potential magma–repository interactions. Mathematical scaling arguments were derived that describe potential decompressive flow processes of gas-bearing and gas-free fluids and agree with laboratory data. Additionally, the effects of these flow patterns developing in viscous fluids on waste package contents were considered. Salient points of these analyses are

- Circulation in a magma-filled drift potentially intersected by a vertical dike was investigated in a series of analog laboratory experiments using a fluid containing various amounts of bubbles. These fluids represent magmas at different stages of degassing [i.e., magmas with no exsolved bubbles (no gas), magmas with a small amount of exsolved bubbles (low gas), and magmas with a moderate amount of exsolved bubbles (high gas)]. In each of these cases, circulation of magma filling the drift was established and driven by either buoyancy differences or viscous coupling.

- In the low and high gas cases, bubbles induce a buoyancy-driven exchange flow between magma in the drift and magma filling/ascending the dike. Bubbly fluid flows from the dike into the drift; bubbles rise and segregate in the horizontal drift, producing a foam at its top and a denser degassed fluid that sinks to its base. Circulation cells are ultimately established in which the influx of bubbly fluid is balanced by the outward flux of foam and degassed fluid into the dike. The length to which the bubbly fluid penetrates the drift and the time scale of gas segregation are both controlled by the rise of bubbles within the drift. Furthermore, in the high gas case, steady-state degassing is associated with periodic foam collapse, which is itself dependent on properties of the foam layer such as thickness.

- The flow of the denser, degassed magma (i.e., a viscous shearing flow) out of the drift into the dike, which might entrain and carry small fragments of spent nuclear fuel toward the surface, depends on the value of the dike/conduit magma supply rate relative to the value of the gas segregation flux. However, the presence of debris on the bottom of drifts would decrease the ability for a return flow to entrain these particles.

- In the no gas case, vortical circulation of magma filling the drift is driven by viscous coupling with the rising magma in the connected dike. The velocity within the drift decreases rapidly with distance away from the intersection with the dike/conduit, suggesting that only very small drag forces will be exerted on the contents of the drift. Buoyancy-driven circulation has a much higher velocity than circulation driven by viscous coupling, and therefore the effects of bubbles in magma dominate exchange flow between magma in the dike/conduit and magma in the drift.

5 REFERENCES

Basu, D., N.K. Adams, J.A. Stamatakos, S. Sparks, and A. Woods. "Review of Two Electric Power Research Institute Technical Reports on the Potential Igneous Processes Relevant to the Yucca Mountain Repository." San Antonio, Texas: CNWRA. 2007.

Bechtel SAIC Company, LLC. "Dike/Drift Interactions." MDL–MGR–GS–000005. Las Vegas, Nevada: Bechtel SAIC Company, LLC. 2004.

Blundy, J., K. Cashman, and M. Humphreys. "Magma Heating by Decompression-Driven Crystallization Beneath Andesite Volcanoes." *Nature*. Vol. 443. pp. 76–80. 2006.

Cashman, K.V. and M.T. Mangan. "Physical Aspects of Magma Degassing II. Constraints on Vesiculation Processes From Textural Studies of Eruptive Products." Mineralogical Society of America. *Reviews in Mineralog*y. Vol. 30. pp. 447–478. 1994.

Cashman, K.V., B. Sturtevant, P. Papale, and O. Navon. "Magmatic Fragmentation in Encyclopedia of Volcanoes." H. Sigurdsson, ed. San Diego, California: Academic Press. pp. 421–430. 2000.

Charru, F., H. Mouilleron, and O. Eiff. "Erosion and Deposition of Particles on a Bed Sheared by a Viscous Flow." *Journal of Fluid Mechanics*. Vol. 519. pp. 55–80. 2004.

Crowe, B., R. Morley, S. Wells, J. Geissman, E. MacDonald, L. McFadden, F. Perry, M. Murrell, J. Poths, and S. Forman. "The Lathrop Wells Volcanic Centre: Status of Field and Geochronology Studies." Proceedings of the Third International Conference for High-Level Radioactive Waste Management, Las Vegas, Nevada, April 12–16, 1992. American Nuclear Society. pp. 1,997–2,013. 1992.

CRWMS M&O. "Miscellaneous Waste-Form FEPs." ANL–WIS–MD–000009. Rev. 00 ICN 01. North Las Vegas, Nevada: DOE, Yucca Mountain Site Characterization Office. 2000.

Duffield, W.A., R.L. Christiansen, R.Y. Koyanagi, and D.W. Peterson. "Storage, Migration, and Eruption of Magma at Kilauea Volcano, Hawaii, 1971–1972." *Journal of Volcanology and Geothermal Research*. Vol. 13. pp. 273–307. 1982.

Fleck, R.J., B.D. Turrin, D.A. Sawyer, R.G. Warren, D.E. Champion, M.R. Hudson, and S.A. Minor. "Age and Character of Basaltic Rocks of the Yucca Mountain Region, Southern Nevada." *Journal of Geophysical Research*. Vol. 101. pp. 8,205–8,227. 1996.

Giordano, D. and D.B. Dingwell. "Non-Arrhenian Multicomponent Melt Vicosity: A Model." *Earth and Planetary Science Letters*. Vol. 208. pp. 337–349. 2003.

Jaupart, C. and S. Vergniolle. "The Generation and Collapse of a Foam Layer at the Roof of a Basaltic Magma Chamber." *Journal of Fluid Mechanics*. Vol. 203. pp. 347–380. 1989.

Lange, R.A. "The Effect of H2O, CO and F on the Density and Viscosity of Silicate Melts." Mineralogical Society of America. *Reviews in Mineralogy*. Vol. 30. pp. 331–369. 1994.

Leeder, M.R. "*Sedimentology and Sedimentary Basins: From Turbulence to Tectonics*." Oxford, United Kingdom: Blackwell. 1999.

Lejeune, A.-M., A.W. Woods, R.S.J. Sparks, B.E. Hill, and C.B. Connor. "The Decompression of Volatile-Poor Basaltic Magma From a Dike into a Horizontal Subsurface Tunnel." San Antonio, Texas: CNWRA. 2002.

Luhr, J.F. and T.B. Housh. "Melt Volatile Contents in Basalts From Lathrop Wells and Red Cone, Yucca Mountain Region (SW Nevada): Insights From Glass Inclusions." *Eos*. American Geophysical Union. Vol. 83. Abstract V22A-1221. 2002.

Menand, T. and J.C. Phillips. "Gas Segregation in Dykes and Sills." *Journal of Volcanology and Geothermal Research*. Vol. 159. pp. 393–408. 2007a.

Menand, T. and J.C. Phillips. "A Note on Gas Segregation in Dykes and Sills at High Volumetric Gas Fractions." *Journal of Volcanology and Geothermal Research*. Vol. 162. pp. 185–188. 2007b.

Menand, T., J.C. Phillips, and R.S.J. Sparks. "Circulation of Bubbly Magma and Gas Segregation Within Tunnels of the Potential Yucca Mountain Repository." *Bulletin of Volcanology*. doi:10.1007/s00445–007–0179–5. 2007.

Nicholis, M.G. and M.J. Rutherford. "Experimental Constraints on Magma Ascent Rate for the Crater Flat Volcanic Zone Hawaiite." *Geology*. Vol. 32. pp. 489–492. 2004.

NRC. NUREG–1762, "Integrated Issue Resolution Status Report." Rev. 2. Vol. 2. Washington, DC: NRC. 2005.

———. "Risk Insights Baseline Report." ML040560162. Washington, DC: NRC. April 2004. <www.nrc.gov/waste/hlw-disposal/reg-initiatives/resolve-key-tech-issues.html>

———. "Issue Resolution Status Report, Key Technical Issue: Igneous Activity." Rev. 2. Washington, DC: NRC, Division of Waste Management. 1999.

Sarda, P. and D. Graham. "Mid-Ocean Ridge Popping Rocks: Implications for Degassing at Ridge Crests." *Earth and Planetary Science Letters*. Vol. 97. pp. 268–289. 1990.

Schlichting, H. "Boundary Layer Theory." New York City, New York: McGraw-Hill. 1960.

Shankar, P.N. and M.D. Deshpande. "Fluid Mechanics in the Driven Cavity." *Annual Review of Fluid Mechanics*. Vol. 32. pp. 93–136. 2000.

Shaw, H.R. "Viscosities of Magmatic Silicate Liquids: An Empirical Method of Prediction." *American Journal of Science*. Vol. 272. pp. 870–893. 1972.

Sparks, R.S.J. "The Dynamics of Bubble Formation and Growth In Magmas: A Review and Analysis." *Journal of Volcanology and Geothermal Research*. Vol. 3. pp. 1–37. 1978.

Sparks, R.S.J. "Dynamics of Magma Degassing." C. Oppenheimer, D.M. Pyle, and J. Barclay, eds. Volcanic Degassing. Geological Society of London Special Publication No. 213. pp. 5–22. 2003.

Vergniolle, S. and C. Jaupart. "Dynamics of Degassing at Kilauea Volcano, Hawaii." *Journal of Geophysical Research*. Vol. 95. pp. 2,793–3,001. 1990.

Woods, A.W. and H.E. Huppert. "On Magma Chamber Evolution During Slow Effusive Eruptions." *Journal of Geophysical Research*. Vol. 108. pp. 12-1 to 12-16. 2003.

Woods, A.W. and R.S.J. Sparks. "Report on Scoping Calculations for Magma-Repository Interaction at Yucca Mountain, Nevada." San Antonio, Texas: CNWRA. 1998.

Woods, A.W., R.S.J. Sparks, O. Bokhove, A-M. LeJeune, C.B. Connor, and B.E. Hill. "Modeling Magma-Drift Interaction at the Proposed High-Level Radioactive Waste Repository at Yucca Mountain, Nevada, U.S.A." *Geophysical Research Letters*. Vol. 29, No. 13. 2002.